

Chloroyttrium 2-(1-(Arylimino)alkyl)quinolin-8-olate Complexes: Synthesis, Characterization, and Catalysis of the Ring-Opening Polymerization of ϵ -Caprolactone

Wenjuan Zhang,[†] Shaofeng Liu,[†] Wenhong Yang,[†] Xiang Hao,[†] Rainer Glaser,^{*,‡} and Wen-Hua Sun^{*,†}

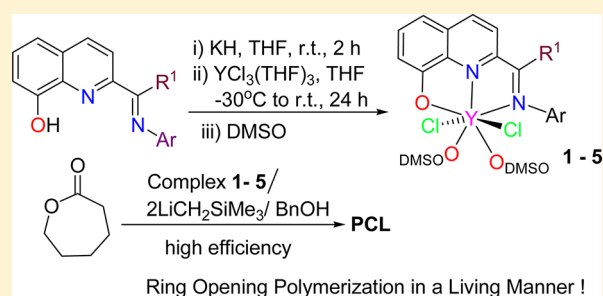
[†]Key Laboratory of Engineering Plastics and Beijing National Laboratory for Molecular Science, Institute of Chemistry, Chinese Academy of Sciences, Beijing 100190, China

[‡]Department of Chemistry, University of Missouri, Columbia, Missouri 65211, United States

S Supporting Information

ABSTRACT: Stoichiometric reactions of $YCl_3(THF)_3$ with potassium 2-((arylimino)methyl)quinolin-8-olates or 2-(1-(arylimino)ethyl)quinolin-8-olates in THF solution gave the mononuclear $LYCl_2(DMSO)_2$ complexes 1–5 in the presence of DMSO and a representative dinuclear complex 6 in the absence of DMSO. All yttrium complexes were fully characterized by NMR measurements and elemental analysis, and the crystal structures of complexes 1 and 4–6 were determined by single-crystal X-ray diffraction. The structures indicate coordination number seven around the yttrium center and pentagonal bipyramidal geometries.

The complexes all feature diapical YCl_2 moieties and one tridentate organic ligand in the equatorial plane. Upon reaction of the yttrium precatalysts 1–6 with $LiCH_2Si(CH_3)_3$ alone or with $LiCH_2Si(CH_3)_3$ together with $BnOH$, the ring-opening polymerization (ROP) of ϵ -caprolactone (ϵ -CL) occurred with high efficiency. Depending on conditions, the ROP of ϵ -CL produced polycaprolactone with narrow molecular distribution and in a living manner. Theoretical studies of the chlorine/ CH_2SiMe_3 and Me_3SiCH_2/BnO ligand exchange reactions suggest that the replacement of the apical ligands can proceed without significantly affecting the equatorial ligands. These results suggest that one of the apical $Y-CH_2SiMe_3$ bonds within the $LY(CH_2SiMe_3)_2$ intermediate catalyzes the polymerization in the $BnOH$ -free process. Most polymers generated by $BnOH$ -assisted catalysis possess M_n values that are similar to $M_{n,cal}$ values based on $Y-OBn$, suggesting that one apical $Y-OBn$ bond of the diapical $LY(OBn)(CH_2SiMe_3)$ intermediate catalyzes most or all of the ring polymerization of ϵ -CL.



INTRODUCTION

Polyesters including polylactide (PLA), polyglycolide (PGL), and polycaprolactone (PCL) are considered "green materials" because they are biocompatible, readily biodegradable, and easily recyclable. Because of these attractive characteristics, the polyesters are used in biomedical and pharmaceutical applications such as drug delivery receptacles, medical bone screws and pins, absorbable surgical sutures, and matrix material for tissue engineering.¹ One convenient method for the synthesis of polyesters consists of the ring-opening polymerization (ROP) of cyclic esters using metal complexes as catalysts or initiators,^{1c,f,2} in which tin and aluminum compounds have been widely used as initiators.³ At the same time, rare earth metal complexes have become attractive catalysts for the ROP of ϵ -CL due to their low toxicity, their rich and diverse coordination chemistry, and their high reactivity.⁴

The triflate salts of some rare earth metals (Sc, Y, Nd, Er) were explored as possible initiators of the ROP of ϵ -CL, and these metals showed low catalytic activity and resulted in polymers with relatively low molecular weights.⁵ In sharp

contrast, yttrium(III) isopropoxide and related heterobimetallic isopropoxides showed high efficiency for polymerization of ϵ -CL and produced polymers with broad molecular distributions ($PDI = 1.4-1.8$).⁶ Among the heterobimetallic isopropoxides, $Sn[Y(O^iPr)_4]_2$ performed better than $Y[Al(O^iPr)_4]_3$ and $Y[Sn(O^iPr)_3]_3$. Moreover, controlled polymerization of ϵ -CL could be achieved by well-defined alkoxy-bridged di- and triyttrium(III) complexes.⁷ For example, tris(phenoxy) yttrium/2-propanol systems were employed for the ROP of ϵ -CL and formed PCL with controlled molecular weight and narrow polydispersity, and moreover some phenoxy yttrium compounds exhibited good controllability for copolymerization of esters.⁸ In the literature, however, it was also reported that $Y(OMe)(C_5Me_5)_2(THF)$ showed no reaction in the ROP of ϵ -CL⁹ and that immobilized yttrium isopropoxides on silica produced only PCL with lower molecular weights ($M_n = 1900$).¹⁰ In contrast, the amide $Y((N(SiMe_3)_2)_3)$ ¹¹ and tris(amidate)yttrium complexes,^{12a-c} activated by alcohols,

Received: August 12, 2012

Published: November 5, 2012

acted as highly effective initiators of the ROP of ϵ -CL and produced PCL with narrow molecular distribution, and these observations suggested yttrium alkoxides as active species.¹¹ Moreover, some alkyl yttrium compounds such as LY-(CH₂SiMe₃)₂ (L: *N*-(8-quinolinyl)-2-(iminomethyl)anilide) caused the ROP of ϵ -CL to proceed in a living fashion.^{13a} Interestingly, bis(phosphino)carbazolide rare earth metal complexes promoted the copolymerization of ϵ -CL with diene.¹⁴ In addition to experimental observation of borohydride yttrium complexes as initiators for the ROP of lactone, the mechanism of this reaction was explored with DFT calculations.¹⁵ These achievements illustrate the high potential of rare earth metal complexes for their applications in ROP catalysis, and it is now a significant goal to find suitable ligands to finely tune the catalytic behavior of their complexes.

Due to their high coordination numbers, rare earth metals were often reported as aggregated (multinuclear) compounds¹⁶ or half-metallocene alkyl complexes.¹⁷ Multidentate organic ligands allow for finely tuning the sizes and electronic properties of the substituents, and these ligands stabilize rare earth metal alkyl compounds.¹⁸ Recently, we prepared 2-(arylimino)quinolin-8-ols and explored their potential as multidentate ligands. Aluminum complexes with these ligands showed high activity in the ROP of ϵ -CL,¹⁹ and their titanium complexes acted as precatalysts for ethylene (co)-polymerization.²⁰ Subsequently, we have been exploring the scope of rare earth metal complexes of these ligands.

Herein the synthesis and characterization of the title complexes are reported along with the results of studies of their catalytic behavior in the ROP of ϵ -CL. Electronic structure theory was also employed to study the putative complexes generated from the precatalysts by chlorine/alkyl and alkyl/alkoxide ligand exchange reactions.

RESULTS AND DISCUSSION

1. Synthesis and Characterization of Yttrium Complexes 1–6. The 2-((arylimino)alkyl)quinolin-8-ol derivatives were prepared according to our reported procedure.¹⁸ Employing the procedure for the synthesis of LTiCl₃ complexes,¹⁸ 2-((2,6-dimethylphenylimino)methyl)quinolin-8-ol was deprotonated with an equivalent amount of potassium hydride in THF, and the potassium salt was used *in situ* to react with an equivalent amount of YCl₃(THF)₃ (Scheme 1). However, we observed some red suspended fine precipitate, which was likely due to aggregation. To increase the solubility of the product, we added several drops of dimethyl sulfoxide (DMSO), a strongly

donating solvent,²¹ and obtained a clear purple solution. Removing the solvent under vacuum, the residue was extracted with CH₂Cl₂ (40 mL) plus drops of DMSO, and the filtrate was concentrated to a volume of about 5 mL solution. Adding 40 mL of Et₂O precipitated a red solid (**1**) in high yield (86%). The compound LYCl₂(DMSO)₂ was characterized by NMR spectroscopy and elemental analysis. Compounds **2–5** were also synthesized in high yields and fully characterized. Comparison of the ¹H NMR spectra of the complexes with the corresponding free ligand shows that the OH resonances around 8.2 ppm disappeared as the M–O bonds formed.

The stoichiometric reaction of potassium 2-((2,6-dimethylphenylimino)methyl)quinolin-8-olate with YCl₃(THF)₃ in DMSO-free solution led to a red suspension and resulted in the formation of an orange compound (**6**) in 46% yield. Its ¹H NMR spectrum showed two sets of ligand peaks with a 1:1 integration ratio, and X-ray diffraction analysis confirmed **6** to be a binuclear complex (*vide infra*).

2. Crystal Structure Analyses. Single crystals of **1** and **4–6** suitable for X-ray structural analysis were grown from dichloromethane/*n*-heptane (**1**, **4**, **5**) or THF/*n*-heptane (**6**) solutions at room temperature. Their selected structural parameters are collected in Table 1, and ORTEP diagrams are displayed in Figures 1–4. We first describe the characteristic structural motifs of these complexes in qualitative terms, and subsequently we will examine some structural relationships quantitatively.

The X-ray structure analyses show monoligated complexes with coordination number 7 for yttrium, and complexes **1**, **4**, and **5** possess very similar geometries around yttrium (Scheme 2). Each yttrium atom within all of the yttrium complexes is coordinated by a tridentate 2-(arylimino)quinolin-8-olate *N,N,O*-ligand in a meridional fashion. For example, in complex **1** shown in Figure 1, the Y metal center is coordinated by the organic tridentate ligand in a meridional mode, by two *trans*-diaxial Cl atoms, and by two *cis*-diequatorial O(DMSO) atoms to generate the 7-fold coordination. The decahedron spanned by the ligands around Y is that of a distorted pentagonal bipyramid. The deviation of Y1 from the equatorial plane is 0.052 Å. The two chelating rings formed by N1, C8, C10, and N2 and by N1, C9, C1, and O1 are essentially coplanar. The crystal structures of **4** and **5** (Figures 2 and 3) show the same coordination motif as in **1**, and the structural parameters agree closely (Table 1).

While the crystal structures of **1** and **4** contain just one molecule in their unit cells, the crystals of **5** contain two independent molecules in the unit cell, and these are numbered **5a** and **5b** in Table 1. The examination of **5a** and **5b** presents an opportunity to examine the sensitivity of the structural parameters to crystal-packing effects, and two parameters stand out. Comparing the values of **5a** and **5b**, one finds that the angles $\angle(\text{Cl}_{\text{ax}}-\text{Y1}-\text{Cl}_{\text{ax}'})$ differ by about 5° and the aryl twists $\angle(\text{C}_{\text{im}}-\text{N}_{\text{im}}-\text{C}_i-\text{C}_o) = \tau$ differ by about 2.5°. Hence, the differences between the $\angle(\text{Cl}_{\text{ax}}-\text{Y1}-\text{Cl}_{\text{ax}'})$ angles of 176.73(4)° (**1**), 176.61(4)° (**4**), 168.36(4)° (**5a**), and 171.18(4)° (**5b**) should not be overinterpreted. The aryl twists τ are 93.3° (**1**), 97.5° (**4**), 93.3° (**5a**), and 95.9° (**5b**), and the situation is similar. The point here is that the twists in all of the Schiff bases place the aryl plane more or less perpendicular to the imine plane, and the exact twist angle is less important because of the small curvature of this internal coordinate.

The binuclear complex **6** does look rather different from **1**, **4**, and **5** at first sight, but its structure in fact shares many of the

Scheme 1. Synthesis of Yttrium Complexes 1–6

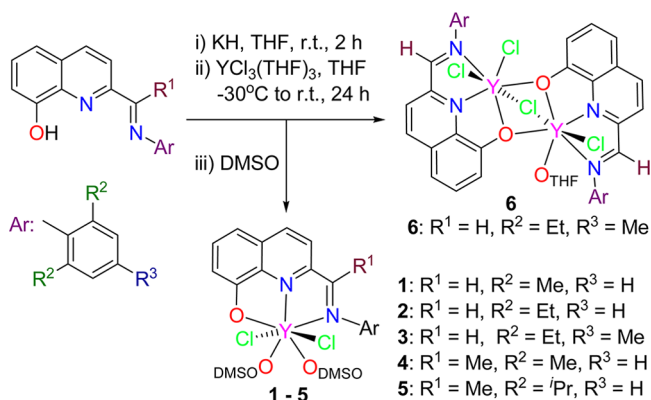


Table 1. Selected Structural Parameters of the Crystal Structures of Yttrium Complexes

parameter	1	4	5a	5b	6.1a	6.1b	6.2a	6.2b
Y–N _{py}	2.429(4)	2.452(4)	2.454(4)	2.440(4)	2.438(6)	2.440(5)	2.442(5)	2.463(5)
Y–N _{im}	2.653(4)	2.665(4)	2.657(4)	2.647(4)	2.619(6)	2.604(5)	2.605(5)	2.626(6)
Y–O(L)	2.238(3)	2.241(3)	2.262(4)	2.248(4)	2.323(4)	2.316(4)	2.380(4)	2.373(4)
Y–O(L')					2.246(4)	2.263(4)	2.318(4)	2.312(4)
Y–O(sol)	2.296(3)	2.296(3)	2.283(4)	2.292(4)	2.397(5)	2.355(5)		
	2.307(3)	2.314(3)	2.275(4)	2.296(4)				
Y1–Cl _{ax}	2.6245(13)	2.6324(14)	2.6033(17)	2.617(2)	2.5490(18)	2.541(2)	2.560(2)	2.5448(19)
Y1–Cl _{ax'}	2.6378(13)	2.6312(14)	2.6459(18)	2.623(2)	2.7149(17)	2.704(2)	2.807(2)	2.772(2)
Y1–Cl _{eq}							2.575(2)	2.5791(18)
Cl _{ax} –Y1–Cl _{ax'}	176.73(4)	176.61(4)	168.36(5)	173.99(6)	175.08(6)	173.90(7)	168.98(5)	164.24(6)
Cl _{ax} –Y–Cl _{eq}							96.63(7)	97.86(7)
Cl _{ax} –Y–Cl _{eq}							88.19(7)	88.25(7)
O1–Y1–N2	131.71(12)	130.81(11)	131.07(13)	132.01(14)	130.50(19)	130.44(15)	128.63(14)	129.89(17)
O1–Y1–N1	68.46(12)	68.28(12)	68.54(14)	69.03(15)	67.03(19)	67.86(16)	66.48(14)	66.15(16)
N1–Y1–N2	63.47(12)	62.64(12)	62.53(13)	63.04(14)	64.2(2)	63.90(18)	63.81(16)	63.95(18)
∠(R1–C _{im} –N _{im})	119.98	125.45	126.05	123.51	118.89	119.21	120.02	118.65
∠(C _{im} –N _{im} –C _i)	116.50	116.63	118.22	118.84	117.27	116.72	115.35	116.25
∠(C _{im} –N _{im} –C _i –C _o)	93.32	97.47	93.32	95.86	110.73	111.73	97.55	102.89

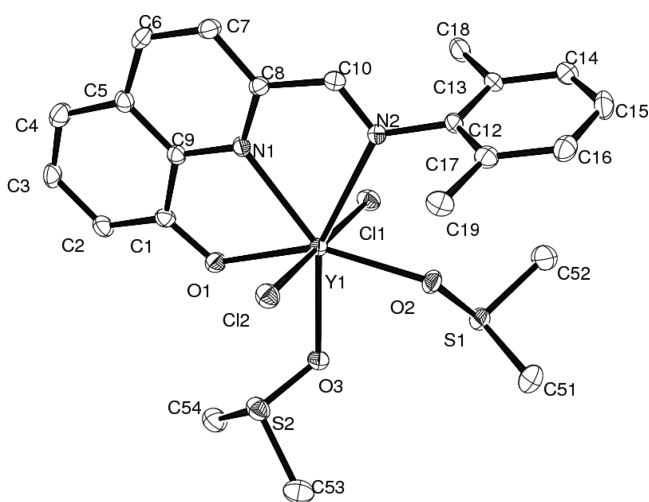


Figure 1. ORTEP drawing of complex 1 with thermal ellipsoids at the 30% probability level. Hydrogen atoms are omitted for clarity.

characteristic features of the mononuclear complexes (Scheme 2): (a) Each yttrium is coordinated by one organic, tridentate ligand L by way of one O and two N atoms in a *mer* arrangement. (b) The coordination number of each yttrium is 7, and each yttrium is located at the center of a trigonal bipyramid. (c) The apical positions are occupied by Cl atoms. The distinguishing features between 1, 4, and 5 and the binuclear complex 6 concern the occupations of the remaining two equatorial positions, which are occupied by DMSO solvent molecules in the mononuclear complexes. It is the first distinguishing feature that the two LYCl₂ moieties are combined such that their phenoxide-O atoms coordinate to both yttrium atoms, and this mode of LYCl₂ interaction fills one of the two available equatorial positions. Second, the two pentagonal bipyramids share one apical chlorine atom (Cl5 in Figure 4), and this feature is important for several reasons. It is one immediate consequence that one chloride becomes available to occupy the last remaining equatorial site around one yttrium (Y2 in Figure 4). It is another important consequence of the shared apical Cl ligand that the base planes of the pentagonal bipyramids are tilted and they enclose an

angle of about 100°. Third, the last remaining equatorial position of the other yttrium (Y1 in Figure 4) is occupied by the O-donor solvent molecule THF. The Y1...Y2 distance of 3.5402(11) Å is similar to those in Y₃(μ₃,η²-OC₂H₄OMe)₂(μ₂,η²-OC₂H₄OMe)₂(μ₂,η¹-OC₂H₄OMe)-(acac)₄.²²

As with 5, the unit cell of 6 contains two symmetry-independent dinuclear complexes, 6a and 6b. Each complex contains two yttrium centers with LYCl₂ (6.1) or LYCl₃ (6.2) moieties, respectively. The pertinent structural parameters of the four LYCl_n moieties are listed in Table 1 together with the averages for the LYCl₂ and LYCl₃ moieties, and these data reveal several significant features. To begin with, there exists a pronounced difference in the Y–Cl_{ax} distances: In 1, 4, and 5, all *d*(Y–Cl_{ax}) values fall in the narrow range 2.60–2.64 Å. In 6, however, the *d*(Y–Cl_{ax'}) values involving a shared chlorine are much longer and more varied (2.70–2.81 Å), while the *d*(Y–Cl_{ax}) bonds to an unshared chlorine are shorter (2.54–2.60 Å). Note in particular that the shared chlorine is significantly farther from the YCl₃ center (2.79 Å) than from the YCl₂ center (2.71 Å). In 6, there also are equatorial chloride ligands, and we note that the *d*(Y–Cl_{eq}) bonds (≈2.58 Å) are slightly longer than the *d*(Y–Cl_{ax}) bonds (≈2.55 Å).

The fusion of two pentagonal bipyramids via a shared O₂Cl face generates a trigonal bipyramidal Y₂O₂Cl core cluster. The two μ₂-O atoms are part of the organic ligands of the LYCl₂ and LYCl₃ moieties, respectively. In Table 1, *d*(Y–O(L)) refers to the Y–O distance between yttrium and the phenoxide-O of ligand L, which also coordinates this yttrium with the N atoms of the very same L ligand. With reference to the *d*(Y–O(L)) values of the mononuclear complexes (2.24–2.26 Å), it is observed that the *d*(Y–O(L)) values in 6 are longer (2.32–2.38 Å), as expected. Of interest is the fact that the *d*(Y–O(L')) bond lengths vary significantly depending on whether the additional coordination is made to an electron-deficient YCl₂ (6.1) or to an electron-rich YCl₃ (6.2) metal center; the former are ~2.25 Å and the latter are ~2.31 Å, respectively.

In all of the complexes, whether mononuclear or binuclear, the distance between Y and the quinoline-N (2.43–2.46 Å) is consistently ~0.2 Å shorter than the distance between Y and the imino-N (2.60–2.66 Å). The same structural phenomenon

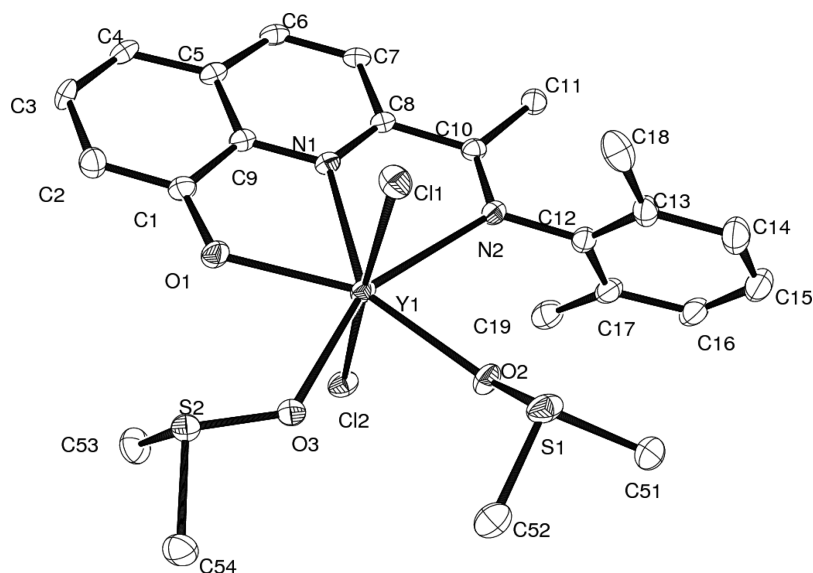


Figure 2. ORTEP drawing of complex 4 with thermal ellipsoids at the 30% probability level. Hydrogen atoms are omitted for clarity.

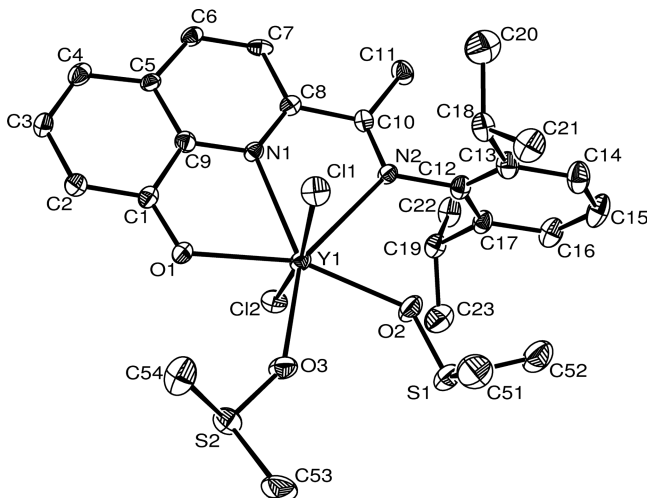


Figure 3. ORTEP drawing of complex 5 with thermal ellipsoids at the 30% probability level. Hydrogen atoms are omitted for clarity. The unit cell contains two independent molecules with similar structures, and only one is shown.

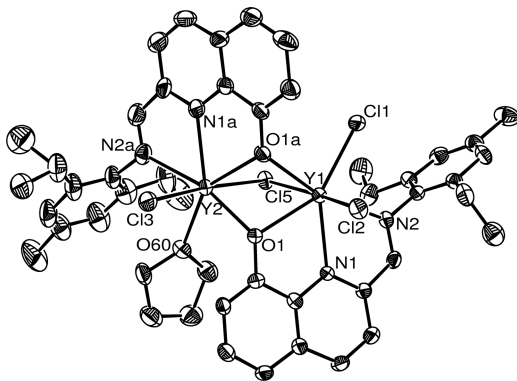


Figure 4. ORTEP drawing of complex 6 with thermal ellipsoids at the 30% probability level. Hydrogen atoms are omitted for clarity. There are two independent molecules in the unit cell, and one of them is illustrated.

Scheme 2. Structural Motifs in Yttrium Complexes 1–5 (left) and 6 (right)



was observed in the titanium analogues bearing the same ligands.²⁰ In the dimeric aluminum analogues,¹⁹ the imino-N is too far away from the Al center to allow for direct bonding.

2. Ring-Opening Polymerization of ϵ -Caprolactone.

Rare earth halides, depending on the reaction parameters, showed verified catalytic activities in the ROP of ϵ -CL that are low²³ or good.²⁴ Previous reports on the use of alkyl yttrium complexes as initiators for the polymerization of cyclic esters^{12,14} showed that the preparation of yttrium alkyl complexes was challenging because of critical problems with their isolation.²⁵ Fortunately, both of these problems have now been overcome because the complexes 1–6 can be purified without any problem. As mentioned before, our group developed a series of trimetallic yttrium complexes that could initiate the high-efficiency ring-opening polymerization of ϵ -CL with or without alcohols.^{12c} Regarding the catalytic property by the title complexes, only a trace amount of polymer was observed in the catalytic system of 1/BnOH, even with variations of the reaction temperature up to 90 °C and reaction times of up to 2 h. ¹H NMR measurement indicated no reaction of the yttrium complex with BnOH and suggested a high stability of the Y–Cl bonds.

Since Y–OBn intermediates are considered to be the active species for ring-opening polymerization of ϵ -CL and inspired by the NaBH₄ initiation reported by the Guillaume group,²⁶ we sought to replace the chloride ligands of complexes 1–6 by reaction with 2 equivalents of the initiator LiCH₂Si(CH₃)₃ to form the catalysts for the ROP of ϵ -CL *in situ*. After initiation with LiCH₂Si(CH₃)₃, the catalytic systems show high catalytic activities for ring-opening polymerization of ϵ -CL.

In order to produce PCLs with narrow molecular weight distributions, it is common practice to employ catalytic

Table 2. ROP of ϵ -CL by 1–6 Initiated by $\text{LiCH}_2\text{Si}(\text{CH}_3)_3/\text{BnOH}^a$

entry	compd	CL:Y:BnOH	t [min]	mg/conv (%)	$M_n^b \times 10^{-4}$	PDI ^b	$M_{n,\text{cal}} \times 10^{-4}$
1	1	500:1:1	5	291 (50.7)	2.83	1.15	2.89
2	1	500:1:1	10	408 (71.0)	3.93	1.18	4.05
3	1	500:1:1	15	478 (83.3)	4.70	1.19	4.75
4 ^c	1	500:1:1	15	561 (97.7)	5.84	1.35	5.62
5 ^d	1	500:1:1	15	570 (99.3)	5.95	1.37	5.70
6	1	250:1:1	30	275 (95.8)	3.16	1.27	2.76
7	1	1000:1:1	30	1117 (97.3)	11.8	1.33	11.2
8	1	2000:1:1	30	2190 (95.4)	22.9	1.37	22.0
9	1	500:1:1	30	547 (95.3)	5.79	1.21	5.48
10	1	500:1:0	30	515 (89.7)	6.57	1.68	5.16
11	2	500:1:1	30	565 (98.4)	5.84	1.14	5.66
12	3	500:1:1	30	560 (97.6)	5.66	1.19	5.62
13	4	500:1:1	30	542 (94.4)	5.20	1.09	5.42
14	5	500:1:1	30	556 (96.9)	6.36	1.28	5.58
15	6	500:1:1	30	544 (94.8)	5.14	1.21	5.46

^aConditions: 10 μmol of Y, 20 μmol of $\text{LiCH}_2\text{Si}(\text{CH}_3)_3$, 1.0 M ϵ -CL toluene solution, 20 °C. ^bGPC data in THF vs polystyrene standards, using correction factor 0.56.²⁸ ^c40 °C. ^d60 °C.

amounts of alcohols.^{4,27} In addition to the screening for optimum polymerization conditions by complex 1 with 2 equivalents of $\text{LiCH}_2\text{Si}(\text{CH}_3)_3$, 1 equivalent of BnOH was added in the successful catalytic system. The results are tabulated in Table 2 (entries 1–9).

Complex 1 was mixed with 2 equivalents of $\text{LiCH}_2\text{Si}(\text{CH}_3)_3$ for 30 min to ensure complete alkylation. One equivalent of BnOH and the prescribed amount of monomer ϵ -CL were added consecutively to initiate the ROP. According to entries 1–3 and 9 in Table 2, a linear relationship was observed (Figure 5) between the monomer conversions and the M_n

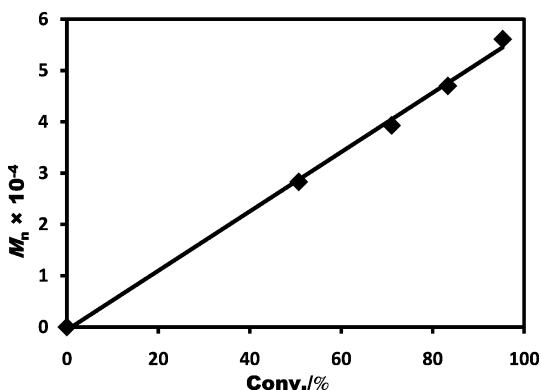


Figure 5. Plot of M_n vs monomer conversion in the ROP of ϵ -CL initiated with 1 as pre-catalyst (entries 1–3 and 9, Table 2).

values with narrow molecular weight distributions (1.15–1.21). This observation suggests that the polymerization happens in a living manner, although the molecular weight distributions of the polymers became slightly broader with increasing reaction time. Assuming that the active species started from the Y–O bond, the M_n values of the polymer products were quite close to the calculated values M_{cal} . The result indicates “single-site” catalytic behavior and is consistent with the performances by dialkyl yttrium complexes or other rare earth metal complexes.^{12a,16} Higher reaction temperatures (entries 4, 5, Table 2) resulted in better conversion and produced PCLs with higher molecular weights with somewhat broader molecular weight

distributions. Nevertheless, most of the resultant PCLs possessed narrow polydispersities with unimodal characteristics.

Changing the ϵ -CL/Y ratios from 250 to 2000 (entries 6–9, Table 2), the molecular weights of the resultant polymers increase approximately linearly with increasing concentration of ϵ -CL (Figure 6). This observation further supports our

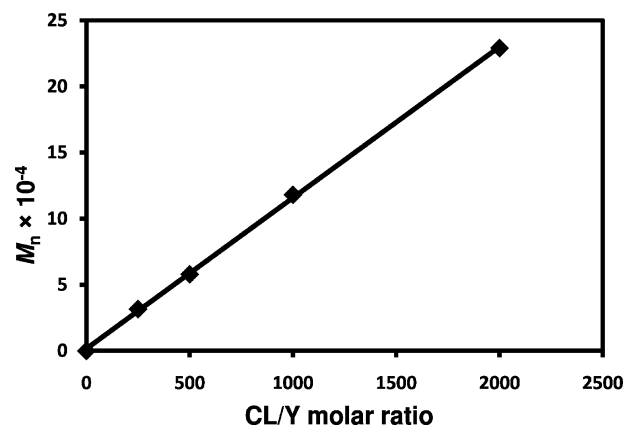


Figure 6. Plots of M_n values vs CL/Y molar ratio in the ROP of ϵ -CL with 1 as pre-catalyst (entries 6–9, Table 2).

proposal that the living polymerization happened within the catalytic system. Moreover, entries 1–3 and 9 in Table 2 show first-order dependence of the polymerization rate on the monomer concentration (Figure 7). The plots in Figures 6 and 7 also suggest that the active species during the ROP of ϵ -CL are not scavenged. All of these results support our proposal of the living polymerization of ROP of ϵ -CL in accordance with the results obtained with dialkyl yttrium complex.^{12a}

The polymerization in the presence of 2 equivalents of $\text{LiCH}_2\text{Si}(\text{CH}_3)_3$ without any BnOH also produced the PCLs, and this result indicates that Y– CH_2SiMe_3 bonds can catalyze the ring-opening polymerization of ϵ -CL. Note, however, that this alcohol-free polymerization is not well behaved and produces PCLs with molecular weights much higher than $M_{n,\text{cal}}$ and with broader PDI values (entry 10, Table 2). The comparatively lower conversion (cf. entry 9, Table 2) indicated either a different type of active species in the absence of BnOH

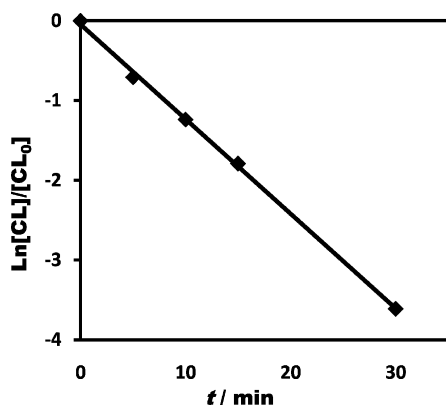


Figure 7. Plots of $\ln[[\text{CL}]/[\text{CL}]_0]$ vs time in the ROP of ϵ -CL with **1** as pre-catalyst (entries 1–3 and 9, Table 2).

or only partial formation of the common active species. Consequently, the yttrium complexes **2–6** were explored with stoichiometric amounts of $\text{LiCH}_2\text{Si}(\text{CH}_3)_3$, one for each chloride, and in the presence of **1** equivalent of BnOH for every yttrium equivalent (1 equiv of BnOH for complexes **2–5**, 2 equiv of BnOH for complex **6**).

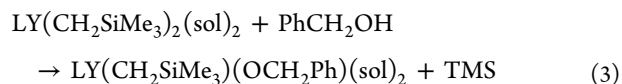
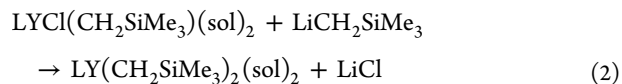
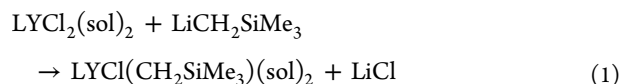
All catalytic systems exhibited very high activity for ROP(CL), demonstrated high degrees of conversion (94.4–98.4%), and produced PCLs with narrow molecular distributions (1.09–1.28). The nature of the organic ligands showed some influence on the catalytic activity of their complexes, but no clear distinctions are manifest between aldimine and ketimine complexes and/or based on the aryl substitution patterns. However, we note that the PCL produced with **5** has a higher molecular weight and broader molecular distribution than PCL produced by the other catalysts. Moreover, the extremely similar activities and polymer characteristics of mononuclear complex **3** and dinuclear complex **6** strongly suggest that both catalysts lead to the same active species.

The ^1H NMR analysis of the resultant polymer (run 9, Table 2) showed the typical signal of $\text{O}-\text{CH}_2\text{Ph}$ (δ 5.10 ppm), suggesting that the $\text{Y}-\text{OCH}_2\text{Ph}$ bond of the active species initiates the polymerization. On the other hand, the narrower distribution of polymers indicated the better controllability by this system with BnOH compared to the BnOH -free process. As mentioned above, most polymers possess M_n values that are similar to $M_{n,\text{cal}}$ based on $\text{Y}-\text{OBn}$, and we interpret this observation to show that only the $\text{Y}-\text{OBn}$ bonds of the $\text{LY}(\text{OBn})(\text{CH}_2\text{SiMe}_3)$ intermediate catalyze the ring polymerization of ϵ -CL, while the $\text{Y}-\text{CH}_2\text{SiMe}_3$ bond does not. A similar observation was made by the Okuda's group, in which the initiation of ϵ -caprolactone ROP by the rare earth cationic $[\text{YMe}(\text{BH}_4)(\text{THF})_5]^+$ occurred by both the borohydride and the methyl group. When the borohydride was replaced by a more electron-donating group of NMe_2 , the *trans*-effect resulted in a higher kinetic facility on the methyl side.^{15a} In addition, the polymerization by the *in situ* catalytic system comprised of **1** and 1 equivalent of $\text{LiCH}_2\text{SiMe}_3$, either with or without 1 equivalent of BnOH produced only trace amounts of polymer. Therefore the monoalkyl monochloro complexes and the monochloro monoalkoxide complexes are inactive in the ring-opening polymerization of ϵ -CL.

The catalytic system generated *in situ* by reaction of **1** with 2 equivalents of $\text{LiCH}_2\text{SiMe}_3$ (path A) did exhibit high catalytic activity. We tried to isolate the dialkyl species but without success. The preparation and isolation of dialkyltitanium

complexes by introduction of the organic ligand into complexes with $\text{Y}-\text{CH}_2\text{SiMe}_3$ bonds also were tried, that is, by adding 1 equivalent of $\text{Y}(\text{CH}_2\text{SiMe}_3)_3(\text{THF})_2$ into a solution of the ligand **L** (path B). These attempts also failed.^{13b} The presumed products formed by paths A and B are thought to be coordination isomers, and the experiments suggest that only one isomer is catalytically active while the other is inert.^{12a,16a} We think that the products of path A are diapical species and that these diapical species are catalytically active. On the other hand, this suggests that dialkyl complexes formed by path B contain two $\text{Y}-\text{CH}_2\text{SiMe}_3$ moieties in a nondiapical arrangement.

3. Theoretical Study of Chlorine/Alkyl and Alkyl/Alkoxide Ligand Exchange Reactions. The described experimental observations suggest that the chemistry of this catalytic system involves the following steps *in situ*. First, alkyl yttrium complexes are generated by successive reactions of the yttrium dichloride complexes with 2 equivalents of $\text{LiCH}_2\text{SiMe}_3$ (eqs 1 and 2) and, second, the dialkyl yttrium complexes are reacted with 1 equivalent of benzyl alcohol per yttrium to generate the yttrium monoalkyl monoalkoxide complex (eq 3), the presumed catalytically active species.



Two equivalents of $\text{LiCH}_2\text{SiMe}_3$ were employed to replace both chloride ligands with carbanions. Unfortunately, all experimental attempts to isolate the dialkyl yttrium complexes failed irrespective as to whether the reactions of complexes **1–5** with 2 equivalents of $\text{LiCH}_2\text{Si}(\text{CH}_3)_3$ were performed at room or low temperature.²⁹

We employed density functional theory (DFT) to investigate the structural feasibility of the $\text{Cl}/\text{CH}_2\text{SiMe}_3$ exchange using the organic ligand **L1** of complex **1**, and the B3LYP/SDD optimized structures are shown in Figure 8.

The hybrid density functional method^{30,31} B3LYP was employed in conjunction with the SDD basis set.³² The optimized structure **M1** shows essentially the same characteristic features that are observed in complex **1** in the crystal structure (Figure 8, top row). As can be seen, packing effects in crystals of **1** merely alter the conformations of one ortho-methyl group and of one DMSO ligand. The structures of **M2** and **M3** show that both the first and the second $\text{Cl}/\text{CH}_2\text{SiMe}_3$ exchanges in the apical positions, respectively, can proceed without major effects on the equatorial ligands. The carbanions are placed above the arene plane of the organic ligand, the planes defined by one Si atom and the C atoms of two of its methyl groups are almost parallel to the arene plane, and the orientations of the two carbanions in **M3** are markedly different relative to the organic ligand. Roughly speaking, the carbanion in **M2** and one of the carbanions in **M3** (the one shown on top in Figure 8) are bonded such that one methyl group is placed above and between N_{im} and N_{py} and one methyl group is placed above and between N_{py} and O_{L1} . This type of carbanion placement (type A) requires avoidance of steric hindrance by

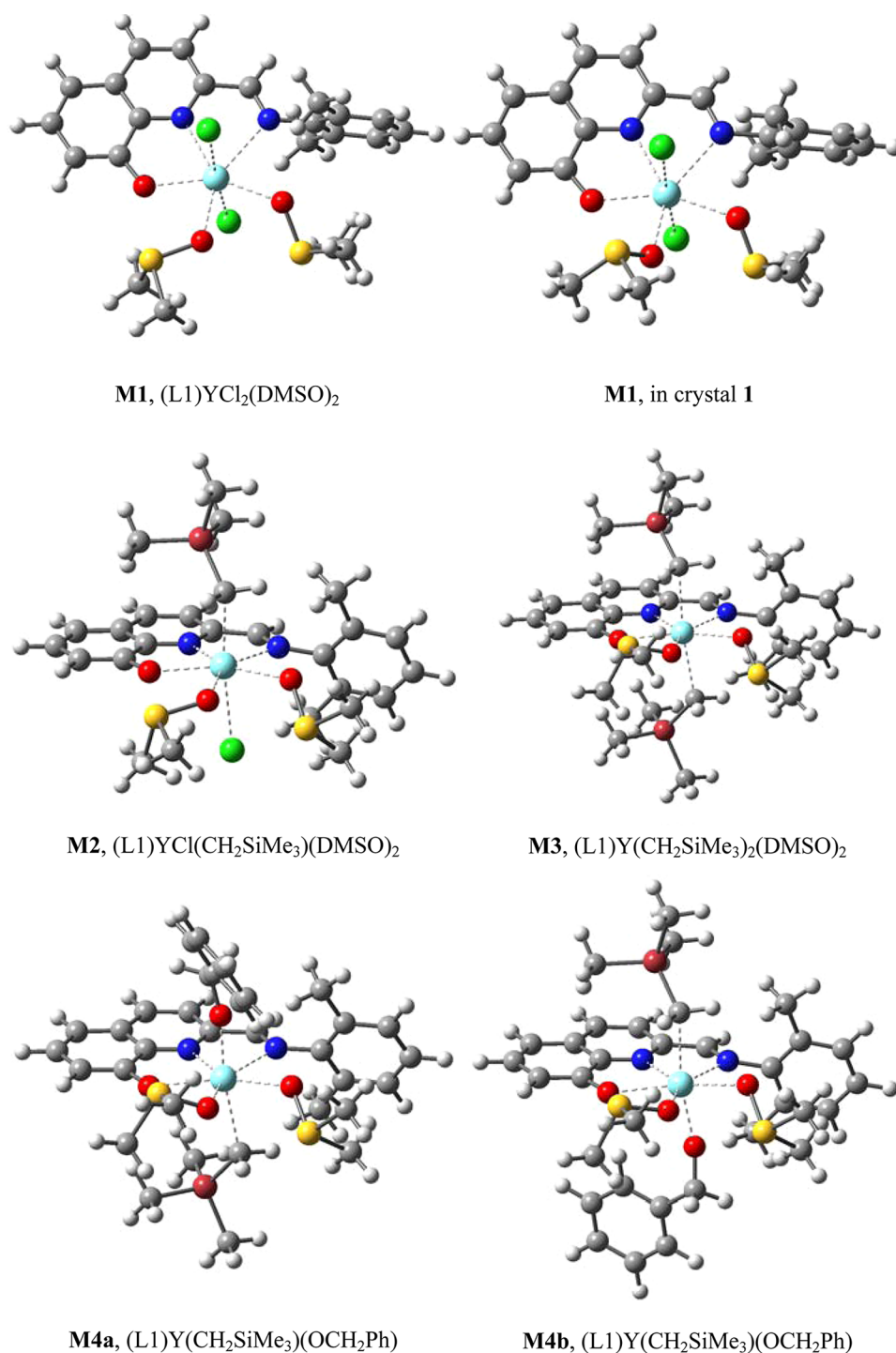


Figure 8. Molecular models of the B3LYP/SDD-optimized structures of complexes M1–M4.

the ortho-alkyl group in the hemisphere occupied by the carbanion and the entire *N*-aryl group is pushed slightly, but markedly into the hemisphere on the other side of the organic ligand. In contrast, the second carbanion in **M3** is bonded such that one methyl group is placed over N_{py} and another methyl group is placed over O_{L1} (type B). It is reasonable to expect the dialkyl complex to be fluxional and that the two nonequivalent alkyl ligands would equilibrate fast even at low temperature.

The packings of the crystal structures of **1** and **4–6** prominently feature parallel stacked arene–arene interactions between the organic ligands of neighboring complexes. Such

crystal packing no longer would be possible with the dialkyl complex **M3**, and it is plausible that it is this feature that has prevented the crystallization of the dialkyl yttrium complexes to date. In the monoalkyl complex **M2**, one arene face of the organic ligand remains accessible to intermolecular arene–arene interactions, and monoalkyl complexes of this type might be more amenable to crystallization and X-ray structure analysis. However, trials to monitor the reaction of the complex with 1 equivalent of $LiCH_2SiMe_3$ could not determine any main product.

Considering that the alkyl groups in **M3** are structurally not equivalent, we optimized two structures, **M4a** and **M4b**, respectively, in which either the type A or the type B carbanion, respectively, was exchanged by the alkoxide ligand BnO^- . Both initial structures were constructed such that the phenyl moiety of the BnO^- ligand had the opportunity to engage in intramolecular arene–arene interactions. Nevertheless, the optimized structure of neither **M4a** nor **M4b** features arene–arene interactions. The benzyl group is placed between the DMSO ligands in **M4a**, and one $\text{C}_{\text{ortho}}\text{--H}$ bond involving of the BnO ligand points directly at the proximate O_{DMSO} (2.916 Å). In **M4b**, the respective $\text{C}_{\text{ortho}}\text{--H}$ bond of the BnO ligand points directly at the phenoxide-O of L1 (2.605 Å). The apical Y--OBn bond lengths are 2.216 Å (**M4a**) and 2.167 Å (**M4b**) and are considerably shorter than the Y--O(L1) bond lengths of 2.347 Å (**M4a**) and 2.350 Å (**M4b**). The apical $\text{Y--CH}_2\text{SiMe}_3$ bond lengths in the dialkyl complex **M3** are 2.543 Å (type A) and 2.569 Å (type B), and the $\text{Y--CH}_2\text{SiMe}_3$ bond lengths in **M4** are very similar, at 2.574 Å (**M4a**, type B) and 2.542 Å (**M4b**, type A). Structure **M4a** is 2.9 kcal/mol more stable than **M4b**.

The vibrational spectra of **M1–M4** were computed, and they are provided as Supporting Information along with overlays of the computed IR spectra of **M1** and **M2**, of **M1** and **M3**, and of **M3** and **M4a**. The $\text{Cl/CH}_2\text{SiMe}_3$ exchange leads to a weak additional band in the low-energy CH stretching region and, most characteristically, to a strong additional band around 930 cm^{-1} (two CH_2SiMe_3 bending modes) in **M3**. The $\text{Me}_3\text{SiCH}_2/\text{BnO}$ exchange leaves the 930 cm^{-1} band essentially in place, while the feature's intensity obviously is reduced. Most characteristically, the reaction of **M3** to **M4** is accompanied by the appearance of two bands around 1100 and 1130 cm^{-1} (BnO bending modes) in a region without strong features of **M3**.

CONCLUSION

The mononuclear compounds **1–5** and the dinuclear complex **6** bearing 2-((arylimino)alkyl)quinolin-8-olate ligands were synthesized and fully characterized. Single-crystal X-ray diffraction analysis established the molecular structures of **1** and **4–6** and demonstrates coordination number 7 around yttrium. Upon reaction with stoichiometric amounts of $\text{LiCH}_2\text{Si}(\text{CH}_3)_3$ (1 equivalent for each chlorine) and of BnOH (1 equivalent for each yttrium), all of these yttrium precatalysts were shown to produce active catalysts that are highly efficient for the ring-opening polymerization of ϵ -caprolactone with a living behavior of polymerization. In most cases, the M_n values of the polymers resulting from the BnOH -assisted polymerization agreed very closely with the calculated values $M_{n,\text{cal}}$ based on one Y--OBn , and this result suggests that the conversions of the precatalysts to the active species are essentially quantitative.

Theoretical studies of the chlorine/ CH_2SiMe_3 and $\text{Me}_3\text{SiCH}_2/\text{BnO}$ ligand exchange reactions suggest that the replacement of the apical ligands can proceed while leaving the equatorial ligands largely unaffected. The computed structure of the dialkyl complex **M3** provides a plausible explanation for the difficulties encountered with the crystallization of the dialkyl yttrium complexes to date: The structure of **M3** impedes intermolecular arene–arene packing interactions, which are thought to be important for crystal packing.

The M_n values of the polymers formed agree well with $M_{n,\text{cal}}$ values calculated based on one $\text{Y--CH}_2\text{Si}(\text{CH}_3)_3$ bond of the

intermediate dialkyl complex of the BnOH -free system or based on the unique Y--OBn bond of the monoalkyl monoalkoxide complex of the BnOH -assisted polymerizations, respectively. The analysis of the BnOH -free process suggests that only one of the apical $\text{Y--CH}_2\text{SiMe}_3$ bonds of the $\text{LY}(\text{CH}_2\text{SiMe}_3)_2$ intermediate catalyzes the polymerization. In the BnOH -assisted process, it is the apical Y--OBn bond of the diapical $\text{LY}(\text{OBn})(\text{CH}_2\text{SiMe}_3)$ intermediate that catalyzes most or all of the ring-opening polymerization, whereas the reactivity of the remaining apical $\text{Y--CH}_2\text{SiMe}_3$ bond in the $\text{LY}(\text{OBn})(\text{CH}_2\text{SiMe}_3)$ intermediate apparently cannot compete.

EXPERIMENTAL SECTION

1. General Procedures. All reactions were performed using standard Schlenk techniques in an atmosphere of high-purity nitrogen or glovebox techniques. Toluene, *n*-heptane, and THF were dried by refluxing over sodium and benzophenone, distilled under nitrogen, and stored over activated molecular sieves (4 Å) for 24 h in a glovebox prior to use. CDCl_3 , DMSO, and C_6D_6 were dried over activated 4 Å molecular sieves. CH_2Cl_2 was dried over CaH_2 for 48 h, distilled under nitrogen, and stored over activated molecular sieves (4 Å) in a glovebox prior to use. $\text{YCl}_3(\text{THF})_3$ was purchased from Aldrich and used as received. Ligands were synthesized according to our reported procedures.^{19,20} Elemental analyses were performed using a PE2400II Series (Perkin-Elmer Co.). ^1H and ^{13}C NMR spectra were recorded on a Bruker DMX-400 (400 MHz for ^1H , 100 MHz for ^{13}C) instrument. All spectra were obtained in the solvent indicated at $25\text{ }^\circ\text{C}$ unless otherwise noted, and chemical shifts are given in ppm and are referenced to SiMe_4 (δ 0.00, ^1H , ^{13}C). The GPC measurements were performed on a set consisting of a Waters-515 HPLC pump, a Waters 2414 refractive index detector, and a combination of Styragel HT-2, HT-3, and HT-4, the effective molar mass ranges of which are 100–10 000, 500–30 000, and 5000–600 000, respectively. THF was used as the eluent (flow rate: 1 mL min^{-1} , at $40\text{ }^\circ\text{C}$). Molecular weights and molecular weight distributions were calculated using polystyrenes as standards.

2. Synthesis of Yttrium Complexes 1–6. Synthesis of 1. To a stirred solution of 2-((2,6-dimethylphenylimino)methyl)quinolin-8-ol (0.145 g, 0.50 mmol) in dried THF (20 mL) at room temperature was added KH (0.020 g, 0.50 mmol). The mixture was allowed to stir for 2 h, and a red solution was obtained. At $-30\text{ }^\circ\text{C}$, $\text{YCl}_3(\text{THF})_3$ (0.206 g, 0.50 mmol) was added, and the resultant mixture was allowed to stir for an additional 24 h at ambient temperature. The residue, obtained by removing the solvent under vacuum, was extracted with CH_2Cl_2 (40 mL) plus drops of DMSO. The filtrate was concentrated *in vacuo* to reduce the volume to 5 mL, and then Et_2O (40 mL) was added to precipitate a red solid. **1** was obtained as a red solid in 86% yield (0.254 g, 0.43 mmol). ^1H NMR (400 MHz, CDCl_3 , $25\text{ }^\circ\text{C}$, TMS): δ 8.53 (s, 1H; CH), 8.43 (d, $^3J(\text{H,H}) = 8.0\text{ Hz}$, 1H; Qin-H), 7.78 (d, $^3J(\text{H,H}) = 7.8\text{ Hz}$, 1H; Qin-H), 7.73 (d, $^3J(\text{H,H}) = 7.8\text{ Hz}$, 1H; Qin-H), 7.64 (t, $^3J(\text{H,H}) = 7.9\text{ Hz}$, 1H; Qin-H), 7.29–7.26 (m, 1H; Qin-H), 7.17 (d, $^3J(\text{H,H}) = 7.8\text{ Hz}$, 2H; Ar-H), 7.14–7.10 (m, 1H; Ar-H), 2.64 (s, 6H; CH_3), 2.55 (s, 12H; DMSO- CH_3). ^{13}C NMR (CDCl_3 , 100 MHz, $25\text{ }^\circ\text{C}$, TMS): δ 168.0, 166.6, 146.1, 145.8, 142.9, 138.9, 132.9, 131.3, 130.0, 127.8, 125.3, 122.7, 112.2, 109.9, 39.5, 21.0. Anal. Calcd for $\text{C}_{22}\text{H}_{27}\text{Cl}_2\text{N}_2\text{O}_3\text{S}_2\text{Y}$: C, 44.68; H, 4.60; N, 4.74. Found: C, 44.22; H, 4.85; N, 4.31.

Synthesis of 2. Using the same procedure for the synthesis of **1**, replacing the ligand with 2-((2,6-diethylphenylimino)methyl)quinolin-8-ol (0.152 g, 0.50 mmol), **2** was obtained as a red solid in 76% yield (0.238 g, 0.38 mmol). ^1H NMR (400 MHz, CDCl_3 , $25\text{ }^\circ\text{C}$, TMS): δ 8.35 (s, 1H; CH), 8.29 (d, $^3J(\text{H,H}) = 8.3\text{ Hz}$, 1H; Qin-H), 7.56 (d, $^3J(\text{H,H}) = 8.3\text{ Hz}$, 1H; Qin-H), 7.46 (t, $^3J(\text{H,H}) = 7.9\text{ Hz}$, 1H; Qin-H), 7.18 (t, $^3J(\text{H,H}) = 7.5\text{ Hz}$, 1H; Ar-H), 7.10 (d, $^3J(\text{H,H}) = 7.5\text{ Hz}$, 2H; Qin-H), 6.92 (d, $^3J(\text{H,H}) = 8.0\text{ Hz}$, 1H; Ar-H), 6.78 (d, $^3J(\text{H,H}) = 7.8\text{ Hz}$, 1H; Ar-H), 2.89–2.80 (m, 4H; CH_2), 2.61 (s, 12H; DMSO- CH_3), 1.10 (t, $^3J(\text{H,H}) = 7.8\text{ Hz}$, 6H; CH_3). ^{13}C NMR (CDCl_3 , 100 MHz, $25\text{ }^\circ\text{C}$, TMS): δ 168.1, 167.0, 150.1, 145.8, 143.2, 139.5, 135.6, 133.4,

131.7, 126.5, 125.6, 123.0, 112.9, 110.4, 40.0, 24.1, 15.6. Anal. Calcd for $C_{24}H_{31}Cl_2N_2O_3S_2Y$: C, 46.53; H, 5.04; N, 4.52. Found: C, 46.15; H, 5.01; N, 4.42.

Synthesis of 3. Using the same procedure for the synthesis of **1**, replacing the ligand with 2-((2,6-dimethyl-4-methylphenylimino)methyl)quinolin-8-ol (0.159 g, 0.50 mmol), **3** was obtained as a red solid in 88% yield (0.279 g, 0.44 mmol). 1H NMR (400 MHz, $CDCl_3$, 25 °C, TMS): δ 8.38 (s, 1H; CH), 8.34 (d, $^3J(H,H) = 8.0$ Hz, 1H; Q_{in}-H), 7.62 (d, $^3J(H,H) = 8.0$ Hz, 1H; Q_{in}-H), 7.71 (d, $^3J(H,H) = 8.0$ Hz, 1H; Q_{in}-H), 7.55 (t, $^3J(H,H) = 7.9$ Hz, 1H; Q_{in}-H), 7.29–7.26 (m, 1H; Q_{in}-H), 6.98 (s, 2H; Ar-H), 3.09–3.04 (m, 2H; CH_2), 2.89–2.81 (m, 2H; CH_2), 2.64 (s, 12H; DMSO- CH_3), 2.29 (s, 3H; CH_3), 1.13–1.27 (m, 6H; CH_3). ^{13}C NMR (100 MHz, $CDCl_3$, 25 °C, TMS): δ 167.9, 166.5, 147.2, 145.4, 142.6, 139.0, 134.9, 134.3, 132.9, 131.2, 126.5, 123.0, 112.4, 110.1, 39.5, 23.6, 21.1, 15.3. Anal. Calcd for $C_{25}H_{33}Cl_2N_2O_3S_2Y$: C, 47.40; H, 5.25; N, 4.42. Found: C, 47.12; H, 5.08; N, 4.22.

Synthesis of 4. Using the same procedure for the synthesis of **1**, replacing the ligand with 2-(1-(2,6-dimethylphenylimino)ethyl)quinolin-8-ol (0.145 g, 0.50 mmol), **4** was obtained as a red solid in 80% yield (0.241 g, 0.40 mmol). 1H NMR (400 MHz, $CDCl_3$, 25 °C, TMS): δ 8.53 (d, $^3J(H,H) = 8.3$ Hz, 1H; Q_{in}-H), 8.43 (d, $^3J(H,H) = 8.3$ Hz, 1H; Q_{in}-H), 8.02 (d, $^3J(H,H) = 8.0$ Hz, 1H; Q_{in}-H), 7.88 (d, $^3J(H,H) = 7.8$ Hz, 1H; Q_{in}-H), 7.57 (t, $^3J(H,H) = 7.8$ Hz, 1H; Q_{in}-H), 7.12–7.07 (m, 2H; Ar-H), 6.85 (d, $^3J(H,H) = 7.7$ Hz, 1H; Ar-H), 2.59 (s, 12H; DMSO- CH_3), 2.40 (s, 3H; CH_3), 2.34 (s, 6H; CH_3). ^{13}C NMR (100 MHz, $CDCl_3$, 25 °C, TMS): δ 167.7, 167.1, 149.5, 146.8, 143.6, 140.1, 137.5, 133.3, 131.1, 126.9, 123.9, 123.1, 113.5, 110.1, 40.6, 18.4, 17.8. Anal. Calcd for $C_{23}H_{29}Cl_2N_2O_3S_2Y$: C, 45.63; H, 4.83; N, 4.63. Found: C, 45.41; H, 5.03; N, 4.36.

Synthesis of 5. Using the same procedure for the synthesis of **1**, replacing the ligand with 2-(1-(2,6-diisopropylphenylimino)ethyl)quinolin-8-ol (0.173 g, 0.50 mmol), **5** was obtained as a red solid in 84% yield (0.272 g, 0.42 mmol). 1H NMR (400 MHz, DMSO- d_6 , 25 °C, TMS): δ 8.68 (d, $^3J(H,H) = 8.6$ Hz, 1H; Q_{in}-H), 8.21 (d, $^3J(H,H) = 8.5$ Hz, 1H; Q_{in}-H), 7.57 (t, $^3J(H,H) = 7.9$ Hz, 1H; Q_{in}-H), 7.25–7.13 (m, 4H; Q_{in}-H and Ar-H), 6.76 (d, $^3J(H,H) = 7.8$ Hz, 1H; Ar-H), 3.03 (sept, $^3J(H,H) = 6.5$ Hz, 2H; CH), 2.35 (s, 3H; CH_3), 1.18 (d, $^3J(H,H) = 6.4$ Hz, 6H; CH_3), 1.01 (d, $^3J(H,H) = 6.6$ Hz, 6H; CH_3). ^{13}C NMR (DMSO- d_6 , 100 MHz): δ 173.4, 166.5, 147.0, 145.3, 142.3, 139.6, 139.0, 132.6, 131.0, 125.6, 123.7, 121.1, 112.7, 110.1, 26.9, 24.7, 24.4, 19.9. Anal. Calcd for $C_{27}H_{37}Cl_2N_2O_3S_2Y$: C, 49.02; H, 5.64; N, 4.23. Found: C, 48.65; H, 5.29; N, 4.13.

Synthesis of 6. To a stirred solution of 2-((2,6-diethyl-4-methylphenylimino)methyl)quinolin-8-ol (0.318 g, 1.00 mmol) in dried THF (30 mL) at room temperature was added KH (0.040 g, 1.00 mmol). The mixture was allowed to stir for 2 h, and a red solution was obtained. At –30 °C, $YCl_3(THF)_3$ (0.412 g, 1.00 mmol) was added, and the resultant mixture was allowed to stir for an additional 24 h at ambient temperature. The residue, obtained by removing the solvent under vacuum, was extracted with CH_2Cl_2 (3 × 20 mL). The combined filtrates were concentrated *in vacuo* to reduce the volume to 5 mL, and then Et_2O (40 mL) was added to precipitate an orange solid (0.236 g, 0.23 mmol, yield 46%). 1H NMR (400 MHz, $CDCl_3$, 25 °C, TMS): δ 8.85 (s, 1H; CH), 8.74 (s, 1H; CH), 8.66 (d, $^3J(H,H) = 8.3$ Hz, 1H; Q_{in}-H), 8.60 (d, $^3J(H,H) = 8.3$ Hz, 1H; Q_{in}-H), 8.13 (d, $^3J(H,H) = 8.2$ Hz, 1H; Q_{in}-H), 8.07 (d, $^3J(H,H) = 8.2$ Hz, 1H; Q_{in}-H), 7.54 (t, $^3J(H,H) = 7.9$ Hz, 1H; Q_{in}-H), 7.46 (t, $^3J(H,H) = 8.3$ Hz, 1H; Q_{in}-H), 7.09–7.6 (m, 2H; Q_{in}-H), 6.99 (s, 2H; Ar-H), 6.97 (s, 2H, Ar-H), 6.72 (d, $^3J(H,H) = 7.8$ Hz, 1H; Q_{in}-H), 6.44 (d, $^3J(H,H) = 7.8$ Hz, 1H; Q_{in}-H), 4.08–3.95 (m, 4H; CH_2), 3.02–2.95 (m, 2H; CH_2), 2.78–2.64 (m, 4H; CH_2), 2.37 (s, 3H; CH_3), 2.35 (s, 3H; CH_3), 2.30–2.20 (m, 2H; CH_2), 1.91–1.89 (m, 4H; CH_2), 1.24–1.13 (m, 12 H; CH_3). ^{13}C NMR ($CDCl_3$, 100 MHz): δ 168.0, 167.5, 166.8, 166.4, 147.0, 146.9, 145.8, 145.3, 143.0, 142.7, 139.6, 138.9, 135.0, 134.6, 134.4, 134.2, 133.0, 132.6, 131.2, 131.1, 126.6, 126.0, 123.2, 122.5, 112.4, 112.3, 110.0, 109.9, 55.0, 23.8, 23.5, 21.1, 20.6, 15.3, 14.9, 13.9. Anal. Calcd for $C_{46}H_{50}Cl_4N_4O_3Y_2$: C, 53.82; H, 4.91; N, 5.46. Found: C, 53.53; H, 4.88; N, 5.13.

3. ROP of ϵ -CL. Typical polymerization procedures in the presence of benzyl alcohol (entry 10, Table 2) are as follows. A toluene solution of **1** (0.010 mmol, 1.0 mL toluene) and $LiCH_2Si(CH_3)_3$ (0.020 mmol) was added into a Schlenk tube in the glovebox at room temperature. The solution was stirred for 30 min, and then BnOH (0.010 mmol) and ϵ -caprolactone (5.0 mmol) along with 3.44 mL of toluene were added to the solution. The reaction mixture was then placed into a water bath at the desired temperature (20 °C), and the solution was stirred for the prescribed time (30 min). The polymerization mixture was then quenched by addition of an excess of glacial acetic acid (0.2 mL) into the solution, and the resultant solution was then poured into filter paper and dried *in vacuo*. Additional ROP of ϵ -CL was carried out by a similar procedure to that described above.

4. Crystal Structure Determinations. Single crystals of **1** and **4–6** suitable for X-ray structural analysis were grown from dichloromethane/*n*-heptane or THF/*n*-heptane solutions at room temperature. Single-crystal X-ray diffraction studies for **4** and **5** was carried out on a Rigaku Saturn 724+ CCD diffractometer with graphite-monochromated Mo $K\alpha$ radiation ($\lambda = 0.71073$ Å), and those of **1** and **6** were carried out on a Rigaku MM007-HF Saturn 724+CCD diffractometer with confocal mirror monochromated Mo $K\alpha$ radiation ($\lambda = 0.71073$ Å). Cell parameters were obtained by global refinement of the positions of all collected reflections. Intensities are corrected for Lorentz and polarization effects and empirical absorption. The structures were solved by direct methods and refined by full-matrix least-squares on F^2 . All non-hydrogen atoms were refined anisotropically. Structure solution and refinement are performed by using the SHELXL-97 package.³³ Crystal data and details are shown in the Supporting Information.

5. Electronic Structure Computations. The DFT computations were performed with the quantum-mechanical software Gaussian 09³⁴ on the SGI Altix system (BX2 NUMA architecture machine with 64 1.5 GHz Intel Itanium2 processors and 128 GB of shared memory) of the Research Supporting Computing facility at the University of Missouri.

■ ASSOCIATED CONTENT

Supporting Information

The crystal data and processing parameters for **1** and **4–6** and their CIF file giving X-ray crystal structural data. Tables with computed energies and thermochemical parameters, Cartesian coordinates of optimized structures, and computed IR spectra. These materials are available free of charge via the Internet at <http://pubs.acs.org>.

■ AUTHOR INFORMATION

Corresponding Authors

* (R.G.) Tel: +1(573) 882-0331. Fax: +1(573) 882-2754. E-mail: GlaserR@missouri.edu. (W.-H.S.) Tel: +86(10) 62557955. Fax: +86(10)62618239. E-mail: whsun@iccas.ac.cn. *

Notes

The authors declare no competing financial interest.

■ ACKNOWLEDGMENTS

This work was supported by NSFC No. 20904059 and the International Exchange Program No. 21110102017.

■ DEDICATION

Dedicated to Professor Christian Bruneau on the occasion of his 60th birthday.

■ REFERENCES

- (1) (a) Arbaoui, A.; Redshaw, C. *Polym. Chem.* **2010**, *1*, 801–826.
- (b) Wu, J.; Yu, T.-L.; Chen, C.-T.; Lin, C.-C. *Coord. Chem. Rev.* **2006**,

- 250, 602–626. (c) Dechy-Cabaret, O.; Martin-Vaca, B.; Bourissou, D. *Chem. Rev.* **2004**, *104*, 6147–6176. (d) Nakano, K.; Kosaka, N.; Hiyama, T.; Nazaki, K. *Dalton Trans.* **2003**, 4039–4050. (e) Stridsberg, K. M.; Ryner, M.; Albertsson, A.-C. *Adv. Polym. Sci.* **2002**, *157*, 41–65. (f) O'Keefe, B. J.; Hillmyer, M. A.; Tolman, W. B. *J. Chem. Soc., Dalton Trans.* **2001**, 2215–2224. (g) Place, E. S.; George, J. H.; Williams, C. K.; Stevens, M. M. *Chem. Soc. Rev.* **2009**, *38*, 1139–1151. (h) Labet, M.; Thielemans, W. *Chem. Soc. Rev.* **2009**, *38*, 3484–3504. (i) Hayashi, T. *Prog. Polym. Sci.* **1994**, *19*, 663–702. (j) Chiellini, E.; Solaro, R. *Adv. Mater.* **1996**, *8*, 305–313.
- (2) (a) Place, E. S.; George, J. H.; Williams, C. K.; Stevens, M. M. *Chem. Soc. Rev.* **2009**, *38*, 1139–1151. (b) Collins, S. *Coord. Chem. Rev.* **2011**, *255*, 118–138.
- (3) (a) Kleawkla, A.; Molloy, R.; Naksata, W.; Punyodom, W. *Adv. Mater. Res.* **2008**, *55–57*, 757–760. (b) Chai, Z.; Zhang, C.; Wang, Z. *Organometallics* **2008**, *27*, 1626–1633. (c) Arbaoui, A.; Redshaw, C.; Hughes, D. L. *Chem. Commun.* **2008**, 4717–4719. (d) Ma, W.-A.; Wang, Z.-X. *Dalton Trans.* **2011**, *40*, 1778–1786. (e) Kowalski, A.; Duda, A.; Penczek, S. *Macromolecules* **2000**, *33*, 689–695. (f) Kowalski, A.; Libiszowski, J.; Biela, T.; Cypriak, M.; Duda, A.; Penczek, S. *Macromolecules* **2005**, *38*, 8170–8176. (g) Schwarz, A. D.; Chu, Z.; Mountford, P. *Organometallics* **2010**, *29*, 1246–1260. (h) Liu, Y.-C.; Ko, B.-T.; Lin, C.-C. *Macromolecules* **2001**, *34*, 6196–6201.
- (4) (a) Platel, R. H. L.; Hodgson, M.; Williams, C. K. *Polym. Rev.* **2008**, *48*, 11–63. (b) Yao, Y. M.; Ma, M.; Shen, Q.; Wong, W. *Organometallics* **2005**, *24*, 4014–4020.
- (5) (a) Möller, M.; Känge, R.; Hedrick, J. L. *J. Polym. Sci., Part A: Polym. Chem.* **2000**, *38*, 2067–2074. (b) Nomura, N.; Taira, A.; Tomioka, T.; Okada, M. *Macromolecules* **2000**, *33*, 1497–1499. (c) Nomura, N.; Taira, A.; Nakase, A.; Tomioka, T.; Okada, M. *Tetrahedron* **2007**, *63*, 8478–8484.
- (6) (a) Deng, X. M.; Zhu, Z.; Xiong, C.; Zhang, L. *J. Appl. Polym. Sci.* **1997**, *64*, 1295–1299. (b) Stevels, W. M.; Ankone, M. J. K.; Dijkstra, P. J.; Feijen, J. *Macromolecules* **1996**, *29*, 8296–8303. (c) Poncelet, O.; Sartain, W. J.; Hubert-Pfalzgraf, L. G.; Folting, K.; Caulton, K. G. *Inorg. Chem.* **1989**, *28*, 263–267.
- (7) Chamberlain, B. M.; Jazdzewski, B. A.; Pink, M.; Hillmyer, M. A.; Tolman, W. B. *Macromolecules* **2000**, *33*, 3970–3977.
- (8) (a) Stevels, W. M.; Ankone, M. J. K.; Dijkstra, P. J.; Feijen, J. *Macromolecules* **1996**, *29*, 3332–3333. (b) Kramer, J. W.; Treitler, D. S.; Dunn, E. W.; Castro, P. M.; Roisnel, T.; Thomas, C. M.; Coates, G. W. *J. Am. Chem. Soc.* **2009**, *131*, 16042–16044.
- (9) Yamashita, M.; Takemoto, Y.; Ihara, E.; Yasuda, H. *Macromolecules* **1996**, *29*, 1798–1806.
- (10) Martin, E.; Dubois, P.; Jérôme, R. *Macromolecules* **2003**, *36*, 7094–7099.
- (11) (a) Martin, E.; Dubois, P.; Jérôme, R. *Macromolecules* **2000**, *33*, 1530–1535. (b) Martin, E.; Dubois, P.; Jérôme, R. *Macromolecules* **2003**, *36*, 5934–5941. (c) Matsuo, Y.; Mashima, K.; Tani, K. *Organometallics* **2001**, *20*, 3510–3518.
- (12) (a) Deng, X.; Yuan, M.; Xiong, C.; Li, X. *J. Appl. Polym. Sci.* **1999**, *73*, 1401–1408. (b) Stanlake, L. J. E.; Beard, J. D.; Schafer, L. L. *Inorg. Chem.* **2008**, *47*, 8062–8068. (c) Zhang, W.; Liu, S.; Sun, W.-H.; Hao, X.; Redshaw, C. *New J. Chem.* **2012**, *36*, 2392–2396.
- (13) (a) Gao, W.; Cui, D.; Liu, X.; Zhang, Y.; Mu, Y. *Organometallics* **2008**, *27*, 5889–5893. (b) Xu, X.; Chen, Y.; Zou, G.; Sun, J. *Dalton Trans.* **2010**, *39*, 3952–3958.
- (14) Wang, L.; Cui, D.; Hou, Z.; Li, W.; Li, Y. *Organometallics* **2011**, *30*, 760–767.
- (15) (a) Susperregui, N.; Kramer, M. U.; Okuda, J.; Maron, L. *Organometallics* **2011**, *30*, 1326–1333. (b) Mahrova, T. V.; Fukin, G. K.; Cherkasov, A. V.; Trifonov, A. A.; Ajjellal, N.; Carpentier, J.-F. *Inorg. Chem.* **2009**, *48*, 4258–4266. (c) Bouyahyi, M.; Ajjellal, N.; Kirillov, E.; Thomas, C. M.; Carpentier, J.-F. *Chem.—Eur. J.* **2011**, *17*, 1872–1883.
- (16) (a) Hayes, P. G.; Welch, G. C.; Emslie, D. J.; Noack, C. L.; Piers, W. E.; Parvez, M. *Organometallics* **2003**, *22*, 1577–1579. (b) Roesky, P. W. *Organometallics* **2002**, *21*, 4756–4761.
- (17) (a) Henderson, L. D.; MacInnis, G. D.; Piers, W. E.; Parvez, M. *Can. J. Chem.* **2004**, *82*, 162–165. (b) Li, X.; Baldamus, J.; Hou, Z. *Angew. Chem. Int. Ed.* **2005**, *44*, 962–965. (c) Zhang, L.; Luo, Y.; Hou, Z. *J. Am. Chem. Soc.* **2005**, *127*, 14562–14563. (d) Jantunen, K. C.; Scott, B. L.; Gordon, J. C.; Kiplinger, J. L. *Organometallics* **2007**, *26*, 2777–2781. (e) Fang, X.; Deng, Y.; Xie, Q.; Moingeon, F. *Organometallics* **2008**, *27*, 2892–2895.
- (18) (a) Shang, X.; Liu, X.; Cui, D. *J. Polym. Sci., Part A: Polym. Chem.* **2007**, *45*, 5662–5672. (b) Tredget, C. S.; Clot, E.; Mountford, P. *Organometallics* **2008**, *27*, 3458–3473.
- (19) Sun, W.-H.; Shen, M.; Zhang, W.; Huang, W.; Liu, S.; Redshaw, C. *Dalton Trans.* **2011**, *40*, 2645–2653.
- (20) Huang, W.; Zhang, W.; Liu, S.; Liang, T.; Sun, W.-H. *J. Polym. Sci., Part A: Polym. Chem.* **2011**, *49*, 1887–1894.
- (21) Linert, W.; Fukuda, Y.; Camart, A. *Coord. Chem. Rev.* **2001**, *218*, 113–152.
- (22) Poncelet, O.; Hubert-Pfalzgraf, L. G.; Daran, J.-C. *Inorg. Chem.* **1990**, *29*, 2883–2885.
- (23) (a) Agarwal, S.; Mast, C.; Anfang, S.; Karl, M.; Dehnicke, K.; Greiner, A. *Polym. Prepr.* **1998**, *39*, 414–415. (b) Shen, Y.; Shen, Z.; Zhang, Y.; Hang, Q. *J. Polym. Sci., Part A: Polym. Chem.* **1997**, *35*, 1339–1352. (c) Shen, Y.; Shen, Z.; Shen, J.; Zhang, Y.; Yao, K. *Macromolecules* **1996**, *29*, 3441–3446.
- (24) (a) Woodman, T. J.; Schormann, M.; Hughes, D. L.; Bochmann, M. *Organometallics* **2004**, *23*, 2972–2979. (b) Agarwal, S.; Karl, M.; Anfang, S.; Dehnicke, K.; Greiner, A. *Polym. Prepr.* **1998**, *39*, 361–362. (c) Chen, H.; Liu, P.; Yao, H.; Zhang, Y.; Yao, Y.; Shen, Q. *Dalton Trans.* **2010**, *39*, 6877–6885. (d) Agarwal, S.; Karl, M.; Dehnicke, K.; Seybert, G.; Massa, W.; Greiner, A. *J. Appl. Polym. Sci.* **1999**, *73*, 1669–1674.
- (25) (a) Luo, Y.; Wang, X.; Chen, J.; Luo, C.; Zhang, Y.; Yao, Y. *J. Organomet. Chem.* **2009**, *694*, 1289–1296. (b) Dugah, D. T.; Skelton, B. W.; Delbridge, E. E. *Dalton Trans.* **2009**, 1436–1445.
- (26) Guillaume, S. M.; Schappacher, M.; Scott, N. M.; Kempe, R. *J. Polym. Sci., Part A: Polym. Chem.* **2007**, *45*, 3611–3619.
- (27) (a) Johnstone, N. C.; Aazam, E. S.; Hitchcock, P. B.; Fulton, J. R. *J. Organomet. Chem.* **2010**, *695*, 170–176. (b) Dunne, J. F.; Manna, K.; Wiench, J. W.; Ellern, A.; Pruski, M.; Sadow, A. D. *Dalton Trans.* **2010**, *39*, 641–653. (c) Shen, M.; Zhang, W.; Nomura, K.; Sun, W.-H. *Dalton Trans.* **2009**, 9000–9009. (d) Pappalardo, D.; Pellicchia, C.; Milano, G.; Mella, M. *Organometallics* **2009**, *28*, 2554–2562. (e) Haddad, M.; Laghzaoui, M.; Welter, R.; Dagonne, S. *Organometallics* **2009**, *28*, 4584–4592. (f) Ma, H.; Spaniol, T. P.; Okuda, J. *Inorg. Chem.* **2008**, *47*, 3328–3339. (g) Gamer, M. T.; Roesky, P. W.; Palard, I.; Hellaye, M. L.; Guillaume, S. M. *Organometallics* **2007**, *26*, 651–657. (h) Shen, M.; Huang, W.; Zhang, W.; Hao, X.; Sun, W.-H.; Redshaw, C. *Dalton Trans.* **2010**, *39*, 9912–9922.
- (28) Save, M.; Schappacher, M.; Soum, A. *Macromol. Chem. Phys.* **2002**, *203*, 889–899.
- (29) (a) Hayes, P. G.; Piers, W. E.; Lee, L. W.; Knight, M. L. K.; Parvez, M.; Elsegood, M. R. J.; Clegg, W. *Organometallics* **2001**, *20*, 2533–2544. (b) Kenward, A. L.; Piers, W. E.; Parvez, M. *Organometallics* **2009**, *28*, 3012–3020. (c) Hou, Z.; Luo, Y.; Li, X. *J. Organomet. Chem.* **2006**, *691*, 3114–3121.
- (30) (a) Sholl, D.; Steckel, J. A. *Density Functional Theory: A Practical Introduction*; Wiley-Interscience: New York, 2009. (b) Koch, W.; Holthausen, M. C. *A Chemist's Guide to Density Functional Theory*, 2nd ed.; Wiley-VCH: Weinheim, 2004.
- (31) Becke, A. D. Density-Functional Thermochemistry. III. The Role of Exact Exchange. *J. Chem. Phys.* **1993**, *98*, 5648–5652.
- (32) (a) Bergner, A.; Dolg, M.; Kuechle, W.; Stoll, H.; Preuss, H. Ab-Initio Energy-Adjusted Pseudopotentials for Elements of Groups 13–17. *Mol. Phys.* **1993**, *80*, 1431–1441. (b) Kaupp, M.; Schleyer, P. v. R.; Stoll, H.; Preuss, H. Pseudopotential Approaches to Ca, Sr, and Ba Hydrides. Why Are Some Alkaline-Earth MX₂ Compounds Bent? *J. Chem. Phys.* **1991**, *94*, 1360–1366. (c) Dolg, M.; Stoll, H.; Preuss, H.; Pitzer, R. M. Relativistic and Correlation Effects for Element 105 (Hahnium, Ha)—A Comparative Study of M and MO (M = Nb, Ta,

Ha) Using Energy-Adjusted *ab Initio* Pseudopotentials. *J. Phys. Chem.* **1993**, *97*, 5852–5859.

(33) Sheldrick, G. M. *SHELXL-97*; University of Göttingen: Göttingen, Germany, 1997.

(34) Frisch, M. J.; Trucks, G. W.; Schlegel, H. B.; Scuseria, G. E.; Robb, M. A.; Cheeseman, J. R.; Scalmani, G.; Barone, V.; Mennucci, B.; Petersson, G. A.; Nakatsuji, H.; Caricato, M.; Li, X.; Hratchian, H. P.; Izmaylov, A. F.; Bloino, J.; Zheng, G.; Sonnenberg, J. L.; Hada, M.; Ehara, M.; Toyota, K.; Fukuda, R.; Hasegawa, J.; Ishida, M.; Nakajima, T.; Honda, Y.; Kitao, O.; Nakai, H.; Vreven, T.; Montgomery, J. A.; Peralta, J. E.; Ogliaro, F.; Bearpark, M.; Heyd, J. J.; Brothers, E.; Kudin, K. N.; Staroverov, V. N.; Keith, T.; Kobayashi, R.; Normand, J.; Raghavachari, K.; Rendell, A.; Burant, J. C.; Iyengar, S. S.; Tomasi, J.; Cossi, M.; Rega, N.; Millam, J. M.; Klene, M.; Knox, J. E.; Cross, J. B.; Bakken, V.; Adamo, C.; Jaramillo, J.; Gomperts, R.; Stratmann, R. E.; Yazyev, O.; Austin, A. J.; Cammi, R.; Pomelli, C.; Ochterski, J. W.; Martin, R. L.; Morokuma, K.; Zakrzewski, V. G.; Voth, G. A.; Salvador, P.; Dannenberg, J. J.; Dapprich, S.; Daniels, A. D.; Farkas, O.; Foresman, J. B.; Ortiz, J. V.; Cioslowski, J.; Fox, D. J. *Gaussian 09*, Revision B.01; Gaussian, Inc.: Wallingford, CT, 2010.